Enhancing and Securing Underwater Optical Wireless Communication Systems Using Identity Row Shift Matrix Code

Somia A. Abd El-Mottaleb
Department of Mechatronics Engineering, Alexandria Higher Institute of Engineering and Technology, Alexandria, Egypt
somaya.ahmed@aiet.edu.eg

Marwa Samara
Department of Electronics and Communications Engineering, Alexandria Higher Institute of Engineering and Technology, Alexandria, Egypt
marwa.samara@aiet.edu.eg

Mehtab Singh
Department of Electronics and Communication Engineering, University Institute of Engineering, Chandigarh University, Mohali 140413, India
mehtab91singh@gmail.com

Hassan Yousif Ahmed
Department of Electrical Engineering, College of Engineering in Wadi Alddawasir, Prince Sattam Bin Abdulaziz University, Wadi Alddawasir, Saudi Arabia
h.ahmed@psau.edu.sa

Median Zeghid
Department of Electrical Engineering, College of Engineering in Wadi Alddawasir, Prince Sattam Bin Abdulaziz University, Wadi Alddawasir, Saudi Arabia
m.zeghid@psau.edu.sa

Abu Sufian A. Osman
Department of Mathematics, College of Science and Humanities in Al-Kharj, Prince Sattam Bin Abdulaziz University, Al-Kharj, Saudi Arabia
a.osman@psau.edu.sa (corresponding author)

Received: 5 January 2026 | Revised: 25 February 2026 | Accepted: 28 February 2026

 DOI: https://doi.org/10.48084/etasr.17362

ABSTRACT

Underwater Optical Wireless Communication (UOWC) systems face challenges of limited transmission range and security, particularly in varying underwater environments characterized by absorption and scattering effects. This paper presents a new approach to enhance and secure UOWC systems by integrating the Identity Row Shift Matrix (IRSM) code. The proposed scheme has been analyzed for its performance across five types of Jerlov waters, demonstrating effective mitigation of channel impairments and enhanced system reliability. Simulation results reveal achievable transmission ranges of 26 m, 23 m, 16.8 m, 10 m, and 4.5 m for Jerlov Types I, IA, IB, II, and III, respectively, under Line-of-Sight (LoS) underwater optical channel conditions. These ranges correspond to received optical power levels of −14.2 dBm, −13.8 dBm, −13.94 dBm, −14.13 dBm, and −14.44 dBm, respectively, while maintaining a Bit Error Rate (BER) below the Forward Error Correction (FEC) threshold of 3.8×10^{-3}. The proposed system achieves a Q-factor exceeding 3, demonstrating reliable multi-user transmission under the adopted channel

mode. Unlike conventional Optical Code Division Multiple Access (OCDMA)-based UOWC systems that rely on Optical Orthogonal Codes (OOC) with non-zero cross-correlation, the proposed IRSM-based scheme employs strictly orthogonal codes with zero cross-correlation, effectively eliminating multi-user interference while embedding physical-layer security directly into the coding structure. This inherent security prevents unauthorized users from decoding the transmitted data without requiring additional encryption or computational overhead. Furthermore, the proposed IRSM/UOWC system supports sustainable underwater monitoring applications by enabling reliable and secure short-range underwater communication, which is critical for environmental monitoring, marine resource management, and supporting sustainable oceanic operations. These findings highlight the potential of the IRSM/UOWC system as a robust solution for high-performance optical communication in diverse underwater environments.

Keywords-Underwater Optical Wireless Communication (UOWC); Identity Row Shift Matrix (IRSM); Jerlov; Q-factor; Bit Error Rate (BER)

I. INTRODUCTION

Underwater Optical Wireless Communication (UOWC) is a nascent domain that utilizes optical technology to enable data transmission in aquatic settings [1]. Conventional communication methods, including acoustic and radio frequency systems, face constraints regarding data rate and range; thus, UOWC presents a viable alternative by employing light waves for high-speed communication. Applications needing high bandwidth, such as video transmission and real-time data streaming, especially benefit from this technology. These applications are essential in several fields, such as environmental monitoring, marine research, and undersea exploration [2, 3].

The principle of UOWC relies on the transmission of modulated light through water, typically using laser diodes or Light-Emitting Diodes (LEDs) as sources [4]. Unlike acoustic systems, which can suffer from low data rates and long propagation delays, optical communication can achieve significantly higher data rates due to the broad spectrum of light frequencies available [5, 6].

In UOWC systems, green light is often preferred over blue due to the unique absorption and scattering behavior of seawater. Although both colors lie within the efficient blue–green wavelength range (roughly 450–550 nm), green light, commonly around 520 nm, experiences lower attenuation and scattering compared to blue light near 450 nm. In turbid waters, such as coastal regions, the optimal transmission wavelength can shift slightly toward 540 nm. This characteristic of green light enhances received optical power and reduces the Bit Error Rate (BER), making it a favorable choice for UOWC applications [7, 8].

However, the underwater environment poses unique challenges that must be addressed to optimize the performance of UOWC systems. These challenges include light absorption and scattering caused by water particles, variations in water clarity, and environmental factors that can affect signal integrity.

Previous studies on LED-based UOWC systems have primarily focused on evaluating link performance under fixed Lambertian radiation patterns, emphasizing the effects of absorption, scattering, and receiver field-of-view on achievable transmission range. However, the impact of optimizing the Lambertian order for beam shaping, particularly in diffuse Line-of-Sight (LoS) underwater scenarios and across different water types, has received limited attention [9].

Additionally, research on UOWC has shown that employing Multiple-Input Multiple-Output (MIMO) architectures can alleviate the adverse effects of absorption, scattering, and optical turbulence. Nevertheless, existing studies often consider a narrow set of modulation schemes, system configurations, or water conditions, leaving a lack of comprehensive assessments that jointly examine MIMO UOWC systems across diverse modulation formats and underwater environments, particularly for Internet of Underwater Things (IoUT) applications [10].

The study in [11] evaluated the performance of multi-hop Optical Wireless Communication (OWC) links by comparing epidemic, depth-based, and focused beam routing protocols under varying underwater conditions, highlighting key trade-offs among reliability, latency, throughput, and scalability.

A comprehensive comparative analysis of multiple modulation schemes using LED- and Laser Diode (LD)-based transmitters at a green wavelength was performed in [12]. The performance in terms of received power, BER, Signal-to-Noise Ratio (SNR), channel capacity, and link range across diverse water types and turbulence conditions was evaluated to highlight the fundamental trade-off between communication range and spectral efficiency in UOWC systems. Moreover, in [13], the authors proposed a Convolutional Neural Network (CNN)-based modulation recognition framework for distinguishing 64-Quadrature Amplitude Modulation (QAM) and 32-Phase Shift Keying (PSK) signals in underwater OWC systems, demonstrating superior classification performance through simulation-based evaluation using standard deep learning metrics.

There are several ways to increase the generalizability of ocean optics by classifying ocean waters based on their optical properties. Jerlov developed the first quantitative categorization technique [14-19], which is based on an apparent optical characteristic of solar downwelling irradiation.

Optical Code Division Multiple Access (OCDMA) is one of the multiplexing techniques that can be used in optical communication networks, allowing several users to use the same optical link concurrently. A unique optical code is given to each user, enabling their data to be encoded into discrete sequences called code words. This encoding guarantees that

even when several people send data at once, their information can be separated and accurately received at the destination based on the unique codes assigned to them [20].

The use of distinct codes also enhances security, as only receivers equipped with the corresponding code can decode the transmitted data. Additionally, OCDMA supports asynchronous access, allowing users to transmit data at different times without requiring synchronization, making it more flexible compared to certain other multiplexing techniques. Utilizing OCDMA in UOWC systems enhances the transmission capacity and provides secure communication [11].

Despite the growing body of literature on UOWC, several important gaps remain. Most existing UOWC studies focus on single-user point-to-point links or evaluate system performance using conventional modulation schemes without addressing scalable multi-user access. While OCDMA has been explored as a potential solution for multi-user UOWC, prior works predominantly rely on Optical Orthogonal Codes (OOC) with non-zero cross-correlation, which introduces multi-user interference and limits both system capacity and physical-layer security. Furthermore, comprehensive evaluations across multiple Jerlov water types using realistic absorption and scattering models are still limited. These gaps motivate the need for a multi-user UOWC framework that simultaneously ensures interference suppression, enhanced security, and robust performance under diverse underwater optical conditions.

The novelty of this work lies in the integration of Identity Row Shift Matrix (IRSM)-based OCDMA into a multi-user UOWC framework evaluated across multiple Jerlov water types using physical-layer performance metrics. Unlike existing UOWC studies that primarily focus on single-user links or employ OOC with non-zero cross-correlation, the proposed approach enables simultaneous multi-user transmission with zero cross-correlation, thereby eliminating multi-user interference while providing inherent physical-layer confidentiality.

This work provides the following key contributions:

- It improves the transmission capacity and provides security to the UOWC system by incorporating three OCDMA users, each utilizing a distinct IRSM code.
- It investigates the effects of different water types, including JI, JIA, JIB, JII, and JIII, on the overall system performance.
- It conducts a comprehensive evaluation of system reliability and efficiency through detailed analyses of received optical power, Q-factor, BER, and eye diagrams.

In addition, the proposed IRSM/OCDMA framework offers inherent physical-layer confidentiality due to the strict orthogonality and zero cross-correlation properties of IRSM codes. Unauthorized receivers without the correct code sequence observe a spectrally spread signal that cannot be deterministically decoded, resulting in BER levels well above the Forward Error Correction (FEC) threshold of 3.8×10^{-3}. Unlike conventional UOWC physical-layer security approaches that rely on beam narrowing, artificial noise injection, or channel state information, the proposed method embeds confidentiality directly within the coding structure while simultaneously enabling multiple-access transmission, without additional power or computational overhead.

IRSM-based OCDMA has been widely investigated in optical fiber communication systems [20], where it has demonstrated strong performance in terms of multi-user capability and interference mitigation. Motivated by these advantages, authors in [21] extended IRSM coding to UOWC for image transmission, considering different underwater environments including pure sea water, clear ocean water, coastal ocean water, and harbor I and harbor II conditions. That study primarily focused on application-layer image quality metrics under varying underwater impairments.

In contrast, the present work addresses a fundamentally different objective. Since image transmission performance does not directly reflect the underlying physical-layer communication limits, this study applies IRSM-based OCDMA to a general UOWC data transmission framework and evaluates its performance across five Jerlov water types. By focusing on physical-layer metrics such as BER, Q-factor, received optical power, and achievable transmission range, the proposed analysis provides deeper insight into the feasibility and scalability of IRSM coding under realistic underwater channel conditions, which cannot be inferred from optical fiber systems or image-based UOWC studies.

The sustainability aspect of the proposed system is discussed from a qualitative, system-level perspective, focusing on moderate transmit power requirements, reduced receiver complexity, and suitability for long-term underwater monitoring applications, rather than through explicit energy-efficiency metrics.

II. ATTENUATION FOR JERLOV WATERS

The world's oceans can be conveniently categorized by their near-surface clarity using Jerlov water types. The Jerlov water classification system divides the ocean into two sections, the open ocean and coastal water. Ten types of Jerlov water are used to describe oceans, ranging from the clearest Jerlov I to the most turbid Jerlov 9C. (I, IA, IB, II, III, 1C, 3C, 5C, 7C, 9C). The open ocean includes IA, IB, II, and III. On the other hand, turbidity is used to classify coastal areas into groups 1–9.

This section discusses the absorption and scattering coefficients for five types of Jerlov waters.

A. Absorption Coefficients

The absorption coefficient in Jerlov waters depends on four terms. The first term is the pure water absorption coefficient, denoted as $\beta_p(\lambda)$, which has a value of 0.0445 m^{-1} at a wavelength, λ, of 532 nm. The second term is the absorption caused by chlorophyll, represented by $\beta_{ph}(\lambda)$, and is expressed as [17]:

$$\beta_{ph}(\lambda) = \mu_{ph}^{J}(\lambda)\left(\frac{\kappa_{ph}}{\kappa_{ph}^{0}}\right)^{0.62} \quad (1)$$

where $\mu_{ph}^{J}(\lambda)$ is chlorophyll spectral absorption [16] and its value is 0.0127 m^{-1} at λ = 532 nm, κ_{ph}^{0} is equal to 1 mg/m^3,

and κ_{ph} is the chlorophyll's overall concentration. Table I shows the values of κ_{ph} in JI, JIA, JIB, JII, and JIII.

TABLE I. THE CONCENTRATION OF CHLOROPHYLL IN JERLOV WATERS [15-18]

Jerlov type	Chlorophyll concentration (mg/m³)
JI	0.03
JIA	0.1
JIB	0.4
JII	1.25
JIII	3

The fulvic acids absorption, $\beta_v(\lambda)$, is the third term and is written as [20]:

$$\beta_v(\lambda) = \mu_v^J(\lambda)\kappa_v \exp(-m_v\lambda) \quad (2)$$

where $\mu_v^J(\lambda)$ is the fulvic spectral absorption and its value is 35.959 m²/mg at λ = 532 nm, m_v is constant with a value of 0.0189 nm⁻¹, κ_v indicates the fulvic acid concentration and is stated in terms of κ_{ph} as [22, 23]:

$$\kappa_v = 1.74098\,\kappa_{ph}\left(\frac{\kappa_{ph}}{\kappa_{ph}^0}\right) \quad (3)$$

Finally, the humic acid absorption, $\beta_u(\lambda)$, is stated as [16]:

$$\beta_u(\lambda) = \mu_u^J(\lambda)\kappa_u \exp(-m_u\lambda) \quad (4)$$

where $\mu_u^J(\lambda)$ is the humic acid spectral absorption and its value is 18.828 m²/mg at λ = 532 nm, m_u is a constant with a value of 0.01105 nm⁻¹, and κ_u is the fulvic acid concentration and is stated in terms of κ_v as [17]:

$$\kappa_u = 0.19334\kappa_{ph}\left(\frac{\kappa_{ph}}{\kappa_{ph}^0}\right) \quad (5)$$

Thus, the Jerlov water's absorption coefficient, $\beta_c(\lambda)$, can be written as [17, 22]:

$$\beta_c(\lambda) = \beta_p(\lambda) + \beta_{ph}(\lambda) + \beta_v(\lambda) + \beta_u(\lambda) \quad (6)$$

Figure 1 presents the absorption coefficient (m⁻¹) for different Jerlov water types. The results show a gradual increase in absorption from clear oceanic waters (JI) to turbid coastal waters (JIII), attributed to higher concentrations of phytoplankton and suspended particles, which leads to increased optical signal attenuation.

B. Scattering Coefficients

The scattering coefficients from small particles, large particles, and pure water are linearly combined to form the scattering coefficient in Jerlov waters, expressed as $\mathbb{S}_c(\lambda)$. The scattering from pure water is stated as [17, 20-27]:

$$\mathbb{S}_{pw}(\lambda) = 0.005826\left(\frac{400}{\lambda}\right)^{4.322} \quad (7)$$

whereas the representation of scattering from small particles is $\mathbb{S}_m(\lambda)$ [18-22], mathematically given as:

$$\mathbb{S}_m(\lambda) = 1.151302\left(\frac{400}{\lambda}\right)^{1.7}\kappa_m \quad (8)$$

where the small particles concentration is κ_m and can be expressed as [17, 20-27]:

$$\kappa_m = 0.01739\kappa_{ph}\exp[0.11631\,(\tfrac{\kappa_{ph}}{\kappa_{ph}^0})] \quad (9)$$

The scattering from large particles is expressed as:

$$\mathbb{S}_b(\lambda) = 0.341100\left(\frac{400}{\lambda}\right)^{0.3}\kappa_b \quad (10)$$

where κ_b is the concentration of large particles in water and can be expressed as [17, 20-27]:

$$\kappa_b = 0.76284\kappa_{ph}\exp\left[0.03092\left(\frac{\kappa_{ph}}{\kappa_{ph}^0}\right)\right] \quad (11)$$

Now, the scattering coefficient, $\mathbb{S}_c(\lambda)$ can be given as:

$$\mathbb{S}_c(\lambda) = \mathbb{S}_{pw}(\lambda) + \mathbb{S}_m(\lambda) + \mathbb{S}_b(\lambda) \quad (12)$$

Figure 2 illustrates the scattering coefficient (m⁻¹) for different Jerlov water types**.** The scattering coefficient increases from clear oceanic waters (JI) to turbid coastal waters (JIII), due to the higher concentration of suspended particles and larger particulate matter in coastal environments, which cause increased optical signal dispersion.

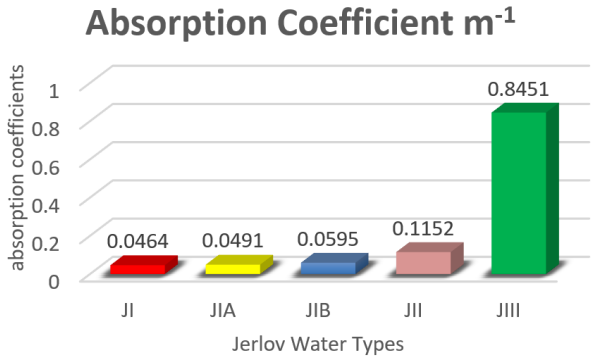

Fig. 1. Absorption coefficients for different Jerlov waters.

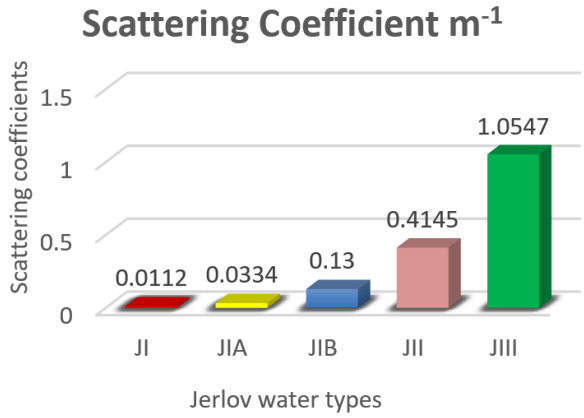

Fig. 2. Scattering coefficients for different Jerlov waters.

III. DESIGN OF PROPOSED IRSM/UOWC SYSTEM

Figure 3 shows the layout of the proposed IRSM/UOWC system. The system includes the following components.

A. Transmitter

At the transmitter, a Pseudo-Random Bit Sequence Generator (PRBSG) is employed to produce 10 Gbps data for each user. The data are then modulated using a Non-Return-to-Zero On-Off Keying (NRZ-OOK) scheme to generate the corresponding electrical signal. In the proposed system, three users are considered, with each user assigned a unique code sequence from the IRSM code family. Assigning unique coding sequences to each user enhances security intrinsically, as the transmitted signal can only be accurately decoded by the intended receiver possessing the corresponding IRSM code.

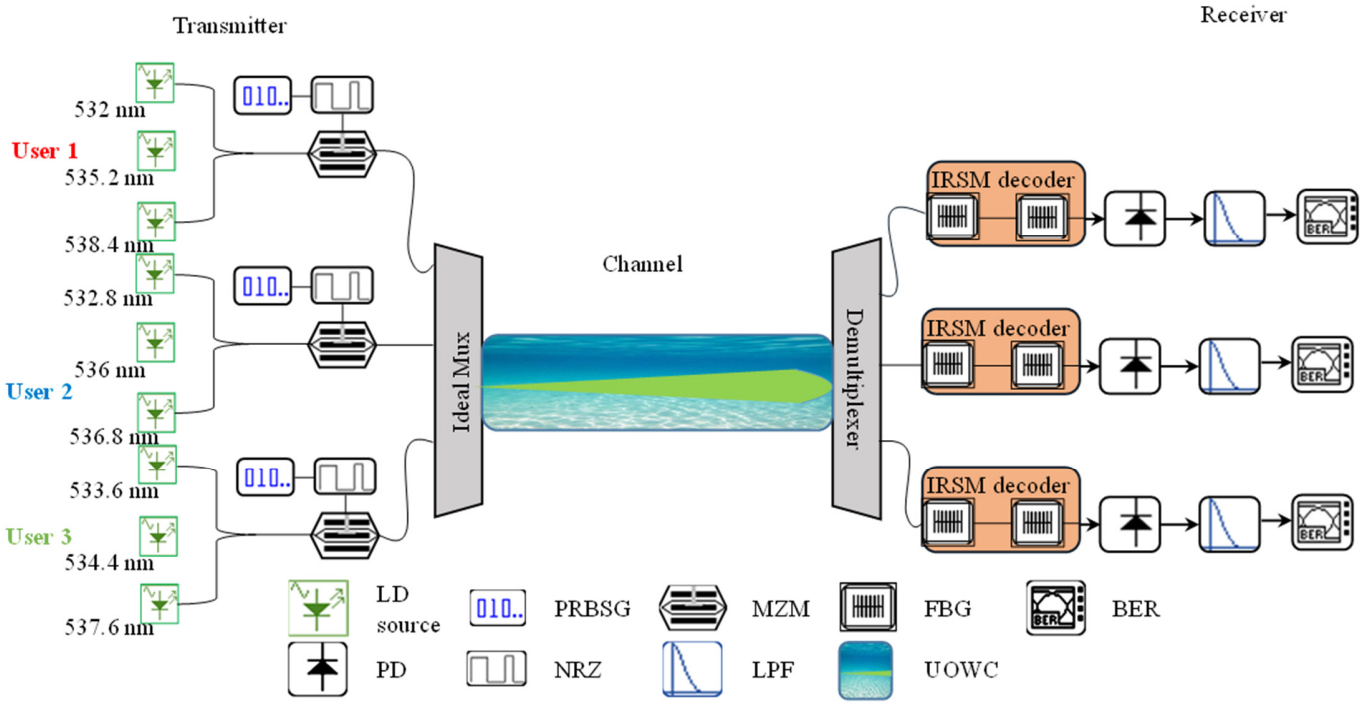

Fig. 3. Layout of the proposed IRSM/UOWC system.

The IRSM code is a type of OCDMA code characterized by zero cross-correlation. The detailed construction of the IRSM code can be found in [20]. For generating optical signals corresponding to IRSM code sequences, LD sources are utilized. The wavelengths corresponding to the assigned IRSM code sequences for the three users are given in Table II. Here, the choice of a green-light wavelength over blue is motivated by the inherent differences in how seawater attenuates these two spectral regions [1, 16].

TABLE II. ASSIGNED IRSM CODE SEQUENCES AND CORRESPONDING WAVELENGTHS FOR USERS

Users	IRSM code sequence	Corresponding wavelengths (nm)
1	100010001	532, 535.2, and 538.4
2	010001100	532.8, 536, and 536.8
3	001100010	533.6, 534.4, and 537.6

To modulate the electrical signal resultant from NRZ-OOK onto the optical signals generated from LD sources, a Mach-Zehnder Modulator (MZM) is utilized. The optical signal from each user is then multiplexed through an ideal Multiplexer (MUX) before travelling in the UOWC channel.

B. Underwater Optical Wireless Communication Channel

The resultant signal from the ideal MUX is then propagated in the UOWC channel. In this paper, a LoS UOWC channel and the attenuations of five types of Jerlov waters are considered.

The received optical power, P_{ROP}, in LoS is expressed as [14, 15]:

$$P_{ROP} = P_{TOP} \cdot G \cdot \eta_{TX} \cdot \eta_{RX} \frac{A_{RX} \cos\theta}{2\pi L^2 [1-\cos\theta_d]} e^{-x(\lambda)L/\cos\theta} \quad (13)$$

where P_{TOP} is the transmitted optical power in dBm, G represents the concentrator gain, and η_{TX} denotes the transmitter optical efficiency. The symbols η_{RX}, A_{RX}, θ, L, and θ_d represent the receiver optical efficiency, receiver aperture area, angle of misalignment between transmitter and receiver, underwater propagation range, and beam divergence angle, respectively. The extinction coefficient, $x(\lambda)$, is expressed as [1, 16]:

$$x(\lambda) = \beta^J(\lambda) + \mathbb{S}_c(\lambda) \quad (14)$$

After propagating through the underwater channel, the signal arrives at the receiver.

C. Receiver

Upon traversing the UOWC channel, the optical signal is first demultiplexed into three separate branches using a demultiplexer. Each branch comprises an IRSM decoder, a Photodiode (PD), a filter, and a BER analyzer. The IRSM decoder employs Fiber Bragg Gratings (FBGs) designed to reflect wavelengths matching those emitted by the LDs at the transmitter, isolating the data-bearing signals for each channel. Subsequently, the optical signal is converted into an electrical signal by the PD. A Low-Pass Filter (LPF) is then applied to suppress any extraneous components. Lastly, the BER analyzer generates the eye diagram of the received data and evaluates the BER.

The resultant current from the PD is expressed as [16, 27]:

$$I = \frac{\Re \cdot P_{ROP} \cdot \omega}{K} \quad (15)$$

where $\Re$ denotes the responsivity of the PD, ω is the code weight of the IRSM code sequence (number of bits '1'), and K is the code length of the IRSM code, expressed as [21]:

$$K = \omega \cdot \mathbb{U} \quad (16)$$

where $\mathbb{U}$ is the number of users.

The SNR can be represented as [15, 21]:

$$\text{SNR} = \frac{\left(\frac{\Re P_{ROP} \omega}{K}\right)^2}{2el\mathcal{B}_e + \frac{4k_B T \mathcal{B}_e}{R_{ld}}} \quad (17)$$

where e denotes the electron charge, k_B is the Boltzmann constant, $\mathcal{B}_e$ refers to the electrical bandwidth of the detector, T represents the receiver's absolute noise temperature, and R_{ld} corresponds to the load resistance of the receiver.

Based on Gaussian approximation, the BER can be expressed in terms of SNR as [15, 16]:

$$\text{BER} = 0.5 erfc\left(\frac{\sqrt{\text{SNR}}}{2\sqrt{2}}\right) \quad (18)$$

where $erfc$ is the complementary error function.

Additionally, BER can be expressed in terms of Q-factor as [11]:

$$\text{BER} = 0.5 erfc\left(\frac{Q}{\sqrt{2}}\right) \quad (19)$$

where the Q-factor can be computed as:

$$Q = \frac{I_1 - I_0}{\sigma_1 + \sigma_2} \quad (20)$$

Here, I_1 and I_0 represent the mean signal levels corresponding to logic "1" and logic "0", respectively, whereas σ_1 and σ_0 are the standard deviations of the noise associated with these levels. This formulation allows the Q-factor to serve as a robust quantitative measure of eye opening and jitter in our analysis.

IV. RESULTS AND DISCUSSION

The proposed IRSM/UOWC system is simulated using Optisystem software (version 22), with the results analyzed and plotted in MATLAB using the parameter values provided in Table III. The system parameters listed in Table III were selected to ensure practical feasibility with commercially available optical components and conservative operational conditions for underwater optical communication.

TABLE III. SYSTEM PARAMETER VALUES [1, 15, 16, 20-24]

Parameter	Value
IRSM encoder	
$\mathbb{U}$	3
ω	3
K	9
Number of LDs per user	3
P_{TOP}	15 dBm
Data generation	
Sequence length of PRBSG	$2^{17}-1$
Data rate	10 Gbps per user
Line encoding scheme	NRZ
Number of channels	4
MZM modulator	
Extinction ratio	25 dB
UOWC channel	
L	JI: 21.5 m to 26 m JIA: 19.5 m to 23 m JIB: 14.5 m to 16.8 m JII: 8.9 m to 10 m JIII: 4.1 m to 4.5 m
η_{TX}	0.9
G	2 dB
θ_d	2 mrad
θ	0°
A_R	31.54 mm2
η_{RX}	0.9
Receiver	
$\Re$	0.8 A/W
$\mathcal{B}_e$	0.75×data rate Hz
T	298 K
R_{ld}	50 Ω

The transmit optical power is set to 15 dBm (≈31.6 mW), which provides adequate link margin to overcome wavelength-dependent absorption and scattering in Jerlov waters while avoiding the need for high-power optical sources. Due to the combined effects of beam divergence and rapid optical attenuation in water, the resulting power density decreases significantly with propagation distance, supporting safe underwater operation.

A data rate of 10 Gbps per user is chosen to meet the requirements of high-bandwidth underwater applications such as real-time video monitoring and dense sensor networks. This data rate is readily supported by standard MZMs and high-speed PDs available in current optical communication systems. The receiver electrical bandwidth is optimized at 0.75× the data rate, following established design guidelines for NRZ signaling formats. This choice balances Inter-Symbol Interference (ISI) mitigation and noise suppression, ensuring reliable signal detection without excessive noise admission.

System performance is evaluated with respect to a pre-FEC BER threshold of 3.8×10^{-3}, which is a widely accepted criterion for reliable communication in optical systems employing hard-decision FEC. The noise model includes shot

noise and thermal noise under the Gaussian approximation, which captures the dominant noise contributions in direct-detection UOWC links. Three users are considered to demonstrate the multi-user capability of the IRSM-based OCDMA scheme while preserving zero cross-correlation and avoiding multi-user interference. Overall, the adopted parameter set reflects realistic, safe, and implementable design choices for practical UOWC deployments.

The results are presented and analyzed in three distinct subsections. The first subsection examines the performance of the received optical power for three users across five different Jerlov water types. The second subsection focuses on the Q-factor performance of the three users in Jerlov water types I, IA, IB, II, and III. Lastly, the third subsection evaluates the BER performance, including eye diagrams for the three users at the maximum achievable underwater link distances for each Jerlov water type. All performance results presented in this section are obtained through numerical simulations conducted using OptiSystem (version 22), with MATLAB employed for data analysis and visualization.

A. Received Optical Power Performance

Figure 4 illustrates the received optical power for the three users in the proposed IRSM/UOWC system. It is evident that the BER performance improves as the received optical power increases for all water types. Conversely, as the underwater link distance increases, the received optical power decreases, leading to a degradation in BER performance. This degradation is physically attributed to the exponential increase in absorption and scattering losses with propagation distance, which reduces the photon count at the receiver and consequently lowers the SNR.

For instance, as shown in Figure 4(a), which presents the BER versus received optical power for JI water, at an underwater link distance of 26 m, the received optical power is −14.26 dBm with a BER of 3.05×10^{-4}. Reducing the propagation distance to 21.5 m increases the received optical power to −9.78 dBm, significantly improving the BER to 6.19×10^{-18}. Additionally, at the maximum underwater link distances of 26 m for JI, 23 m for JIA, 16.8 m for JIB, 10 m for JII, and 4.5 m for JIII, the corresponding received optical powers are −14.2 dBm, −13.8 dBm, −13.94 dBm, −14.13 dBm, and −14.44 dBm, respectively. Moreover, the longest transmission distances are achieved in JI, which exhibits the lowest absorption and scattering coefficients.

Table IV summarizes the received optical power for the three users at link distances of 26 m, 23 m, 16.8 m, 10 m, and 4.5 m for JI, JIA, JIB, JII, and JIII waters, respectively.

TABLE IV. RECEIVED OPTICAL POWER FOR JI, JIA, JIB, JII, AND JIII WATERS AT LINK DISTANCES OF 26 M, 23 M, 16.8 M, 10 M, AND 4.5 M, RESPECTIVELY

Water type (range)	Received optical power (dBm)		
	User 1	User 2	User 3
JI (26 m)	−14.206	−14.206	−14.206
JIA (23 m)	−13.818	−13.818	−13.818
JIB (16.8 m)	−13.949	−13.949	−13.949
JII (10 m)	−14.132	−14.132	−14.132
JIII (4.5 m)	−14.440	−14.440	−14.440

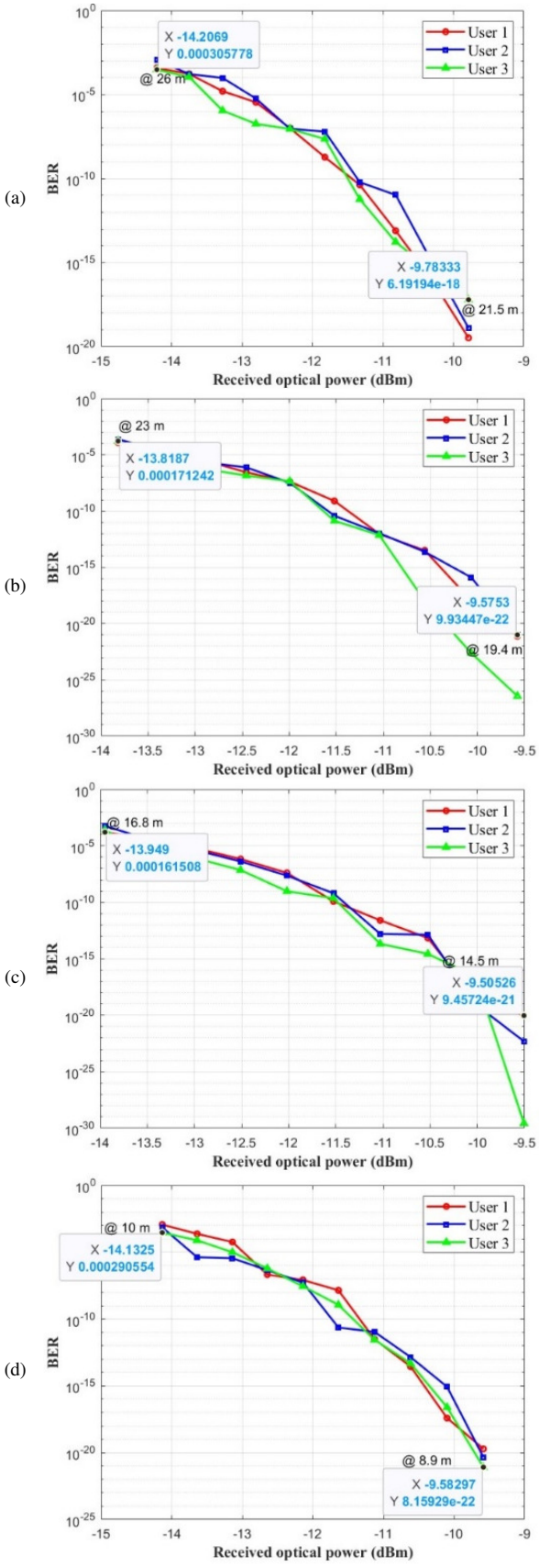

(e)

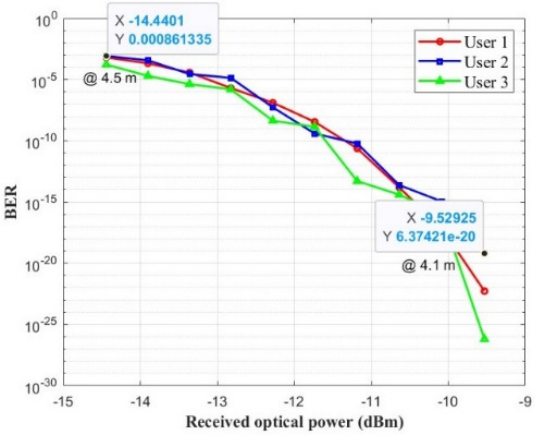

Fig. 4. BER versus received optical power for three users of the proposed IRSM/UOWC system in: (a) JI, (b) JIA, (c) JIB, (d) JII, and (e) JIII.

B. Q-Factor Performance

Figure 5 depicts the Q-factor performance of the three users in the proposed IRSM/UOWC system, each carrying information at 10 Gbps and assigned unique IRSM code sequences, as a function of underwater link distances for five types of Jerlov water that have different optical characteristics.

The results reveal a decline in Q-factor performance as the separation between the transmitter and receiver increases. For instance, in JIA for user 3, the Q-factor decreases from 8.54 to 3.4 as the underwater span increases from 21.5 m to 26 m.

(a)

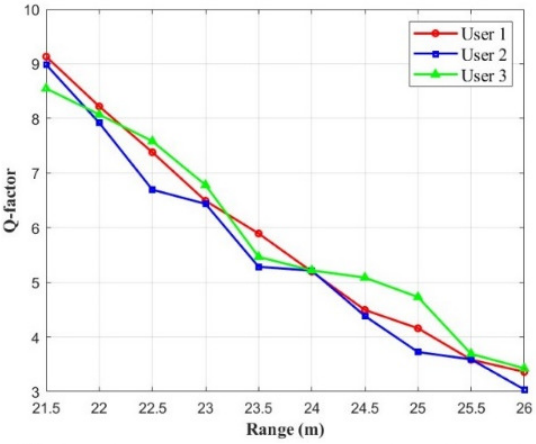

(b)

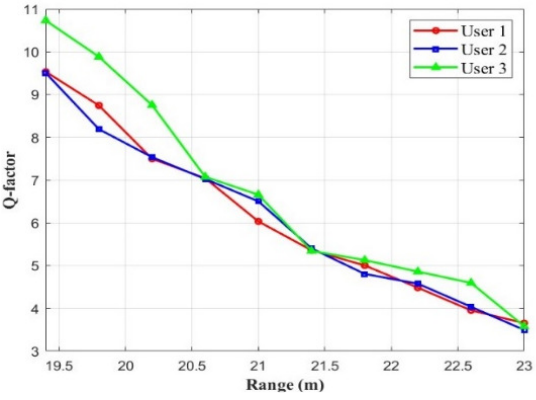

(c)

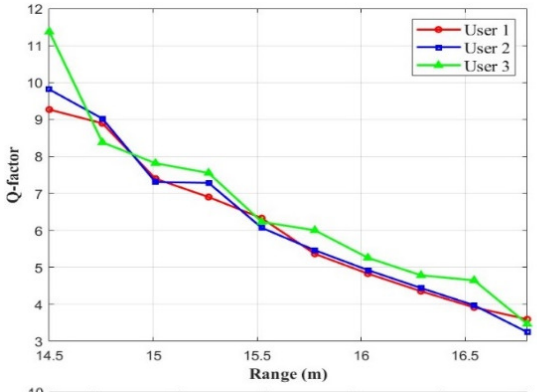

(d)

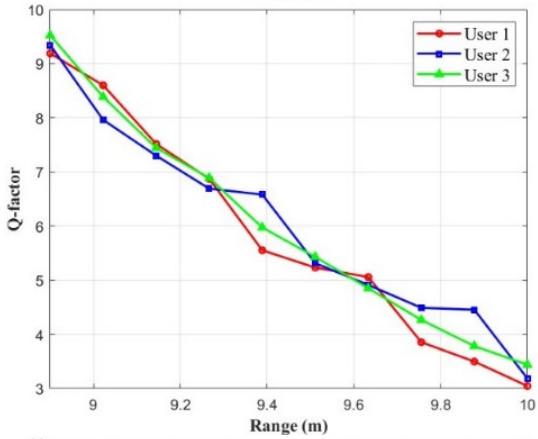

(e)

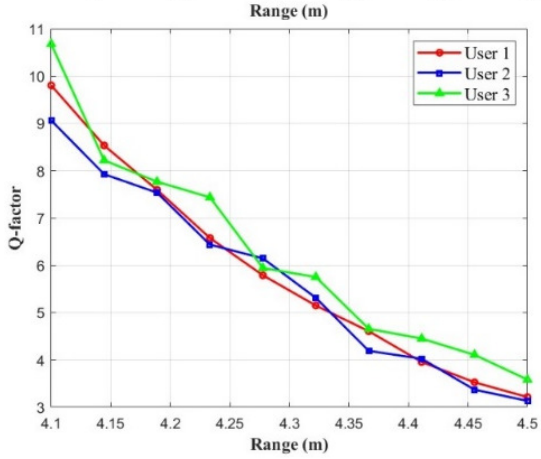

Fig. 5. Q-factor versus received optical power for three users of the proposed IRSM/UOWC system in: (a) JI, (b) JIA, (c) JIB, (d) JII, and (e) JIII.

Notably, all three users achieve a maximum underwater link distance of 26 m in JI water with a Q-factor of approximately 3 (Figure 5(a)). This superior performance is attributed to the low attenuation coefficient in JI water.

In comparison, a moderate underwater propagation range of 23 m is achieved in JIA water at the same Q-factor (Figure 5(b)). This reduced range is due to the slightly higher attenuation coefficient of JIA water relative to JI water. JIB water has a higher attenuation coefficient than both JI and JIA, further impeding optical signal transmission. Consequently, the maximum underwater distance in JIB water as shown in Figure 5(c) is limited to 16.8 m, which is 9.2 m shorter than JI water

and 6.2 m shorter than JIA water at a Q-factor of approximately 3. The shortest underwater spans of 10 m and 4.5 m are observed in Jerlov water types II and III, respectively, at a Q-factor of approximately 3. These restricted ranges are attributed to the elevated levels of dissolved organic matter and suspended particles in these enclosed waters resulting in significantly higher attenuation coefficients, $x(\lambda)$, leading to reduced eye opening and higher noise variance at the receiver.

Table V summarizes the Q-factor for the three users at 26 m, 23 m, 16.8 m, 10 m, and 4.5 m for JI, JIA, JIB, JII, and JIII waters, respectively.

TABLE V. Q-FACTOR FOR JI, JIA, JIB, JII, AND JIII WATERS AT LINK DISTANCES OF 26 M, 23 M, 16.8 M, 10 M, AND 4.5 M, RESPECTIVELY

Water type (range)	Q-factor		
	User 1	User 2	User 3
JI (26 m)	3.362	3.039	3.426
JIA (23 m)	3.654	3.495	3.580
JIB (16.8 m)	3.596	3.248	3.469
JII (10 m)	3.046	3.186	3.440
JIII (4.5 m)	3.213	3.134	3.583

C. Bit Error Rate Performance

Figure 6 demonstrates the BER performance of three users assigned with three distinct IRSM codes for the proposed system across various underwater ranges in five different water environments (JI, JIA, JIB, JII, and JIII). One can notice that there is a clear positive correlation between underwater transmission distance and BER, highlighting the detrimental effect of increased underwater propagation range on system performance. The most significant attenuation is observed in JIII water (1.8998 m^{-1}), resulting in a maximum range of only 4.5 m with BER below 10^{-4}.

In contrast, the superior transmission characteristics of JI water, attributable to its low absorption and scattering coefficients, allowed for a maximum range of 26 m, substantially exceeding the ranges in other water types at a similar BER. JIA, JIB, and JII waters yielded intermediate ranges of 23 m, 16.8 m, and 10 m, respectively. Figures 6(a-e) display the eye diagrams for the three users at these maximum ranges (26 m, 23 m, 16.8 m, 10 m, and 4.5 m for JI, JIA, JIB, JII, and JIII, respectively). The wide eye openings in these diagrams confirm successful reception of the total transmitted data rate of 30 Gbps.

Table VI summarizes the BER for the three users at 26 m, 23 m, 16.8 m, 10 m, and 4.5 m for JI, JIA, JIB, JII, and JIII waters, respectively.

TABLE VI. BER FOR JI, JIA, JIB, JII, AND JIII WATERS AT LINK DISTANCES OF 26 M, 23 M, 16.8 M, 10 M, AND 4.5 M, RESPECTIVELY

Water type (range)	BER		
	User 1	User 2	User 3
JI (26 m)	3.8×10^{-4}	1.1×10^{-3}	3.1×10^{-4}
JIA (23 m)	1.2×10^{-4}	2.3×10^{-4}	1.7×10^{-4}
JIB (16.8 m)	1.6×10^{-4}	5.7×10^{-4}	2.6×10^{-4}
JII (10 m)	1.1×10^{-3}	7.1×10^{-3}	2.9×10^{-3}
JIII (4.5 m)	6.5×10^{-3}	8.6×10^{-3}	1.6×10^{-3}

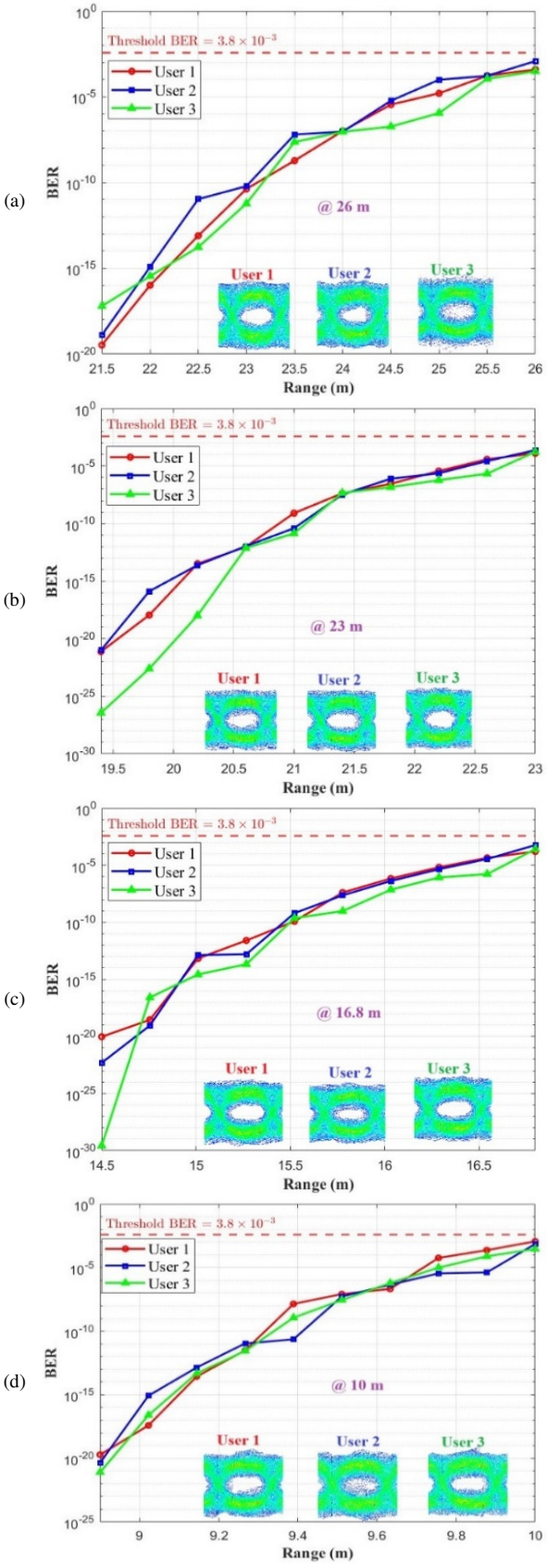

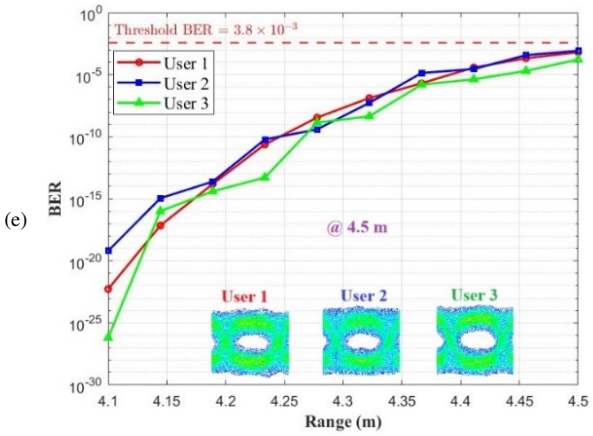

Fig. 6. BER versus underwater range for three users of the proposed IRSM/UOWC system in (a) JI, (b) JIA, (c) JIB, (d) JII, and (e) JIII.

D. Comparative Analysis with Existing UOWC Techniques

While this study primarily quantifies physical-layer reliability through BER, Q-factor, and transmission range, the proposed IRSM/UOWC architecture offers significant advantages for practical underwater deployment regarding data rate, complexity, and energy efficiency. The system supports a high aggregate data rate of 30 Gbps, making it well-suited for bandwidth-intensive applications such as real-time high-definition video monitoring.

From a complexity and energy perspective, the reliance on passive optical components, specifically FBGs for code generation and decoding, eliminates the need for high-speed, power-consuming Digital Signal Processing (DSP) often required for complex modulation or electronic equalization. This all-optical processing approach not only reduces the computational burden and electrical power consumption of the underwater nodes, which is critical for battery-operated marine networks, but also ensures minimal system latency by avoiding the processing delays inherent in electronic conversion and iterative algorithms.

Although the proposed IRSM/UOWC system is evaluated through simulations, the adopted channel modeling closely reflects real underwater optical conditions by employing absorption and scattering coefficients based on the experimentally validated Jerlov water classification. This ensures accurate representation of the dominant wavelength-dependent attenuation mechanisms in practical UOWC links.

Table VII presents a comparison between representative UOWC techniques reported in the literature and the proposed IRSM-based system. Existing approaches rely on conventional modulation or coding schemes and are typically limited either in transmission range or in multi-user capability. In contrast, the proposed IRSM scheme inherently supports multiple users with zero cross-correlation, which significantly mitigates multi-user interference while maintaining competitive transmission ranges. This embedded coding-based security and scalability distinguish the proposed system from conventional UOWC solutions.

TABLE VII. COMPARISON BETWEEN THE PROPOSED SYSTEM AND PREVIOUS WORKS

Reference	[15]	[28]	[29]	Proposed system
Technique	OCDMA using OOC	Pulse Position Modulation (PPM)	Manchester coding	OCDMA using IRSM
Wavelength	532 nm	550 nm	470 nm	532 nm
Optical source	LED	LED	LED	LD
Water type	Pure sea, clear ocean, and coastal ocean	JI, JIA, and JIB	Harbor water	JI, JIA, JIB, JII, and JIII
Underwater distance	27.9 m for pure sea, 17.1 m for clear, and 11.15 for coastal	25 m for JI, 20 m for JIA, and 10 m for JIB	10 m	26 m for JI, 23 m for JIA, 16.8 m for JIB, 10 m for JII, and 4.5 m for JIII
Data rate	NA	NA	10 Mbps	30 Gbps
Multi-user support	Yes (limited by cross-correlation)	No	No	Yes

E. Robustness Under Mobility and Dynamic Underwater Conditions

The performance evaluation in this work assumes an ideal LoS alignment to characterize the fundamental performance limits of the proposed IRSM-based OCDMA scheme under different Jerlov water conditions. In practical underwater environments, platform mobility, water currents, and mechanical vibrations may introduce beam misalignment and beam wandering, resulting in additional geometric power losses and fluctuations in the received optical power.

Despite these non-ideal conditions, the simulation results indicate that the proposed IRSM/UOWC system operates with a substantial link margin at nominal transmission distances. For example, in JI water at a propagation distance of 21.5 m, the system achieves a BER of 6.19×10^{-18}, which is several orders of magnitude lower than the FEC threshold of 3.8×10^{-3}. This margin allows the system to tolerate moderate pointing errors or turbulence-induced fading before performance degradation becomes critical.

Time-varying scattering and turbulence may also cause temporal dispersion and ISI in underwater optical channels. Compared to uncoded OOK transmission, the IRSM-based OCDMA architecture offers improved resilience by enabling spectral discrimination at the receiver, which helps suppress uncorrelated and delayed signal components. Although severe dynamic conditions would reduce the achievable transmission range, the proposed system is expected to maintain reliable performance under moderate underwater mobility and channel variations.

In LoS UOWC scenarios over short to moderate distances, attenuation effects dominate system performance, whereas turbulence-induced fading has a comparatively limited impact. The proposed IRSM-based OCDMA scheme with NRZ-OOK and direct detection provides inherent robustness to moderate power fluctuations, as performance is primarily governed by received optical power and SNR.

Practical impairments such as transmitter–receiver misalignment, ambient light noise, and hardware non-idealities are partially accounted for through beam divergence, misalignment parameters, and noise modeling in the BER analysis. Moreover, spectral decoding using FBGs improves immunity to ambient light interference. The proposed framework is hardware-agnostic and can be readily implemented using commercially available UOWC components.

V. CONCLUSION

This study demonstrated the effectiveness of integrating the Identity Row Shift Matrix (IRSM) code into Underwater Optical Wireless Communication (UOWC) systems to enhance both performance and security in challenging underwater environments. The system's performance was thoroughly evaluated across five Jerlov water types (JI, JIA, JIB, JII, and JIII), demonstrating its capability to mitigate channel impairments and maintain reliable data transmission. A comprehensive analysis, including metrics such as Q-factor, Bit Error Rate (BER), and eye diagrams, was conducted for the three users of the proposed system. Simulation results showed achievable transmission ranges of 26 m, 23 m, 16.8 m, 10 m, and 4.5 m for the respective water types, with received optical power levels ranging from −14.2 dBm to −14.44 dBm. The system consistently maintained a BER below the Forward Error Correction (FEC) threshold of 3.8×10^{-3} and a Q-factor above 3, ensuring robust and high-quality communication.

For future work, the proposed IRSM-based UOWC framework can be extended to explicitly incorporate underwater optical turbulence effects, including beam wander and scintillation, to assess system robustness under dynamic channel conditions. Further capacity enhancement can be achieved by integrating additional multiplexing techniques, such as Orbital Angular Momentum (OAM) beam multiplexing, alongside IRSM-based Optical Code Division Multiple Access (OCDMA). These extensions are particularly relevant for practical underwater applications, including environmental monitoring networks, autonomous underwater vehicles, and secure short-range underwater data links within Internet of Underwater Things (IoUT) systems.

ACKNOWLEDGMENT

The authors extend their appreciation to Prince Sattam bin Abdulaziz University for funding this research work through project number PSAU/2025/01/34620.

FUNDING STATEMENT

This research was funded by Prince Sattam bin Abdulaziz University, grant number PSAU/2025/01/34620.

REFERENCES

[1] H. Kaushal and G. Kaddoum, "Underwater Optical Wireless Communication," *IEEE Access*, vol. 4, pp. 1518–1547, 2016, https://doi.org/10.1109/ACCESS.2016.2552538.

[2] P. S and C. M. Denny J, "An efficient approach to detect and segment underwater images using Swin Transformer," *Results in Engineering*, vol. 23, Sept. 2024, Art. no. 102460, https://doi.org/10.1016/j.rineng.2024.102460.

[3] S. T, R. S, S. J, J. S. R. Alex, R. G, and M. Das, "Reinforcement learning-based automated modulation switching algorithm for an enhanced underwater acoustic communication," *Results in Engineering*, vol. 23, Sept. 2024, Art. no. 102791, https://doi.org/10.1016/j.rineng.2024.102791.

[4] J. Nie *et al.*, "Adaptive beam shaping for enhanced underwater wireless optical communication," *Optics Express*, vol. 29, no. 17, pp. 26404–26417, Aug. 2021, https://doi.org/10.1364/OE.434387.

[5] M. F. Ali, D. N. K. Jayakody, Y. A. Chursin, S. Affes, and S. Dmitry, "Recent Advances and Future Directions on Underwater Wireless Communications," *Archives of Computational Methods in Engineering*, vol. 27, no. 5, pp. 1379–1412, Nov. 2020, https://doi.org/10.1007/s11831-019-09354-8.

[6] A. Shaw, A. i. Al-Shamma'a, S. R. Wylie, and D. Toal, "Experimental Investigations of Electromagnetic Wave Propagation in Seawater," in *2006 European Microwave Conference*, Manchester, UK, 2006, pp. 572–575, https://doi.org/10.1109/EUMC.2006.281456.

[7] L. K. Gkoura *et al.*, "Underwater Optical Wireless Communication Systems: A Concise Review," in *Turbulence Modelling Approaches - Current State, Development Prospects, Applications*, K. Volkov, Ed. London, UK: IntechOpen, 2017, pp. 219–236, https://doi.org/10.5772/67915.

[8] X. Chen *et al.*, "150 m/500 Mbps Underwater Wireless Optical Communication Enabled by Sensitive Detection and the Combination of Receiver-Side Partial Response Shaping and TCM Technology," *Journal of Lightwave Technology*, vol. 39, no. 14, pp. 4614–4621, July 2021, https://doi.org/10.1109/JLT.2021.3077086.

[9] M. M. Zayed, M. Shokair, S. Elagooz, and H. Elshenawy, "Link budget analysis of LED-based UWOCs utilizing the optimum Lambertian order (OLO)," *Optical and Quantum Electronics*, vol. 56, no. 9, Aug. 2024, Art. no. 1396, https://doi.org/10.1007/s11082-024-07341-3.

[10] M. M. Zayed, M. Shokair, and S. Elagooz, "Underwater optical MIMO for high data-rate IoUT," *Journal of Optics*, Feb. 2025, https://doi.org/10.1007/s12596-025-02493-1.

[11] M. M. Zayed, M. Shokair, S. Elagooz, and H. Elshenawy, "Multihop optical wireless underwater communication links utilizing various routing protocols for IoUT applications," *Journal of Optics*, Oct. 2024, https://doi.org/10.1007/s12596-024-02290-2.

[12] M. M. Zayed and M. Shokair, "Performance analysis and optimization of modulation techniques for underwater optical wireless communication in varied aquatic environments," *Scientific Reports*, vol. 15, no. 1, Sept. 2025, Art. no. 32570, https://doi.org/10.1038/s41598-025-18406-y.

[13] M. M. Zayed, S. Mohsen, A. Alghuried, H. Hijry, and M. Shokair, "IoUT-Oriented an Efficient CNN Model for Modulation Schemes Recognition in Optical Wireless Communication Systems," *IEEE Access*, vol. 12, pp. 186836–186855, 2024, https://doi.org/10.1109/ACCESS.2024.3515895.

[14] S. M. Hameed, A. A. Sabri, and S. M. Abdulsatar, "Filtered OFDM for underwater wireless optical communication," *Optical and Quantum Electronics*, vol. 55, no. 1, Dec. 2022, Art. no. 77, https://doi.org/10.1007/s11082-022-04359-3.

[15] M. M. Al Hammadi and Md. J. Islam, "Performance evaluation of underwater wireless optical CDMA system for different water types," *Photonic Network Communications*, vol. 39, no. 3, pp. 246–254, June 2020, https://doi.org/10.1007/s11107-020-00886-9.

[16] S. A. A. El-Mottaleb, M. Singh, A. Atieh, and M. H. Aly, "Performance evaluation of a UOWC system based on the FRS/OCDMA code for different types of Jerlov waters," *Applied Optics*, vol. 63, no. 3, pp. 762–771, Jan. 2024, https://doi.org/10.1364/AO.507674.

[17] P. Singh, K. Chaitanya, Sonali, A. Dixit, and V. K. Jain, "Study of Performance Enhancement in Underwater Optical Wireless Communication System," in *2020 IEEE International Conference on Advanced Networks and Telecommunications Systems*, New Delhi, India, 2020, pp. 1–6, https://doi.org/10.1109/ANTS50601.2020.9342759.

[18] A. Vavoulas, H. G. Sandalidis, and D. Varoutas, "Underwater Optical Wireless Networks: A k-Connectivity Analysis," *IEEE Journal of Oceanic Engineering*, vol. 39, no. 4, pp. 801–809, Oct. 2014, https://doi.org/10.1109/JOE.2013.2291135.

[19] W. H. W. Hassan, N. B. Sanmugam, F. Jasman, and Md. R. Awal, "Experimental Study on the Effect of Water Salinity in the Underwater Optical Wireless Communication (UOWC) Channel," *Journal of Communications*, vol. 19, no. 9, pp. 433–440, Jan. 2024, https://doi.org/10.12720/jcm.19.9.433-440.

[20] M. Alayedi, A. Cherifi, A. Ferhat Hamida, B. S. Bouazza, and C. B. M. Rashidi, "Performance Enhancement of SAC-OCDMA System Using an Identity Row Shifting Matrix Code," in *Proceedings of International Conference on Information Technology and Applications*, Dubai, UAE, 2021, pp. 547–559, https://doi.org/10.1007/978-981-16-7618-5_48.

[21] S. A. Abd El-Mottaleb, A. Atieh, and M. H. Aly, "Next-generation UOWC enabling high-speed and secure RGB image transmission using IRSM-OCDMA with PSO-based image enhancement," *Scientific Reports*, vol. 15, no. 1, Dec. 2025, Art. no. 44130, https://doi.org/10.1038/s41598-025-30710-1.

[22] M. M. Zayed, M. Shokair, S. Elagooz, and H. Elshenawy, "A more detailed mathematical model for analyzing the link budget in UWOCs for both LoS and N-LoS scenarios," *Journal of Optics*, Sept. 2024, https://doi.org/10.1007/s12596-024-02220-2.

[23] M. M. Zayed and M. Shokair, "Modeling and simulation of optical wireless communication channels in IoUT considering water types turbulence and transmitter selection," *Scientific Reports*, vol. 15, no. 1, Aug. 2025, Art. no. 28381, https://doi.org/10.1038/s41598-025-10935-w.

[24] M. M. Zayed and M. Shokair, "Performance analysis of 450/520 nm LD-PS based UOWC systems for IoUT applications across various water conditions using opti-system," *Optical Review*, vol. 32, no. 5, pp. 684–704, Oct. 2025, https://doi.org/10.1007/s10043-025-01002-w.

[25] V. I. Haltrin, "Chlorophyll-based model of seawater optical properties," *Applied Optics*, vol. 38, no. 33, pp. 6826–6832, Nov. 1999, https://doi.org/10.1364/AO.38.006826.

[26] R. C. Smith and K. S. Baker, "Optical properties of the clearest natural waters (200–800 nm)," *Applied Optics*, vol. 20, no. 2, pp. 177–184, Jan. 1981, https://doi.org/10.1364/AO.20.000177.

[27] C. Gabriel, M.-A. Khalighi, S. Bourennane, P. Léon, and V. Rigaud, "Monte-Carlo-Based Channel Characterization for Underwater Optical Communication Systems," *Journal of Optical Communications and Networking*, vol. 5, no. 1, pp. 1–12, Jan. 2013, https://doi.org/10.1364/JOCN.5.000001.

[28] M. A. A. Ali and F. Kh. Shaker, "Performance of an underwater non-line-of-sight (NLOS) wireless optical communications system utilizing LED," *Journal of Optics*, vol. 53, no. 2, pp. 1429–1437, Apr. 2024, https://doi.org/10.1007/s12596-023-01289-5.

[29] G. Cossu *et al.*, "Sea-Trial of Optical Ethernet Modems for Underwater Wireless Communications," *Journal of Lightwave Technology*, vol. 36, no. 23, pp. 5371–5380, Dec. 2018, https://doi.org/10.1109/JLT.2018.2871088.